Bulgarian Journal of Physics vol. **48** (2021) 432–440

Shape Evolution in Ge, Se, Kr and Sr Nuclei within the Covariant Density Functional Theory

M. El Adri, M. Oulne

High Energy Physics and Astrophysics Laboratory, Department of Physics, Faculty of Sciences SEMLALIA, Cadi Ayyad University, P.O.B. 2390, Marrakesh, Morocco

Received *5 October 2021*

Abstract. A systematic study of the shape evolution in Ge ($Z = 32$), Se ($Z = 34$), Kr ($Z = 36$) and Sr ($Z = 38$) isotones for $N = 70$, and their neighboring isotones with $N = 68$ and $N = 72$ is presented. We use, in this investigation, the covariant density functional theory (CDFT) with the explicit Density Dependent Meson-Exchange (DD-ME2) and Density-Dependent Point-Coupling (DD-PC1) models. The finite range pairing interaction separable in coordinate space which was proposed by Tian et al. has been used to treat the pairing correlations. By investigating structural properties of nuclei under consideration, it is found that $N = 70$ isotones are, in generally, spheric. Furtheremore, the $N = 70$ can be considered as magic number.

KEY WORDS: Ge, Se, Kr and Sr isotopes; Nuclei far from the stability; Covariant Density Functional Theory (CDFT); Shape evolution.

1 Introduction

Experimental and theoretical studies of nuclei far from stability are at the forefront of nuclear science. Therefor, a reliable study of such nuclei requires a consistent theory that can describe nuclei in both ground and excited states. In this context, many nuclear approaches have emerged. Among these, the ab-initio [1–4] and shell-model methods which are successfully used in description of light nuclei. However, the complexity of calculations has limited the application of ab-initio method in medium, heavy and super-heavy ones, whereas significant progress has been reported in the development of shell-model techniques which use sophisticated truncation schemes [5] to predict the properties of heavier nuclei. Nowadays, with the mean-field concept, the microscopic approaches based on nuclear Energy Density Functionals (EDFs) are the most accurate tools

that can be applied in all over the nuclear chart including those very close to drip lines. Generally, there are three classes of nuclear EDFs: the Skyrme energy functional [6–8], the Gogny effective interaction [9] and the relativistic mean-field model [10, 11], which are widely used today and capable to compete with the micro-macroscopic method on a quantitative level.

Recently, many studies indicate that Covariant Density Functional Theory (CDFT) is quite reliable and accurate in analysing and describing the nuclear structure, not only in nuclei lying at the valley of stability, but also in those located far from it, which are usually dubbed "exotic nuclei", as it has been proved in Refs [12–16]. In 2019, S. Sharma and al. [17] have studied, within Covariant Density Functional Theory, the deformation and occurrence of shape transitions with change of neutron number in $^{104-144}$Te isotopes. In the super-heavy region, recent study [18] predict $N = 172$ and 184 as spherical magic with DD-ME2 interaction in $Z = 122$ isotopic series.

In the present work, we employ the relativistic EDFs, also called Covariant Density Functional Theory (CDFT), with two classes, namely: Density Dependent Meson-Exchange (DD-ME) and Density Dependent Point-Coupling (DD-PC) parameters in order to investigate the shape evolution in the exotic region. The paper is organized as follows: Section 2 shortly outlines the approach that we have used to do our calculations. In Section 3 numerical tests as well as the input details and the interactions used in calculations are presented. The obtained results are analysed and discussed in Section 4. Finally, the main conclusions are given in Section 5.

2 Theoretical Framework

Covariant Density Functional Theory (CDFT), also often labelled as relativistic Hartree-Bogoliubov (RHB) theory, is a microscopic theoretical tool that can be used to describe the entire nuclear chart with success. In the present work, we have employed two classes of relativistic Hartree-Bogoliubov theories. The first one is the DD-PC model [19, 20] which is characterised by a zero-range interaction and the second one is the DD-ME model [21] which uses a finite interaction range. A brief description of these models is given in the following subsections.

2.1 The Density-Dependent Meson-Exchange

The basic building blocks of relativistic Hartree-Bogoliubov for DD-ME is the standard Lagrangian density with medium dependent vertice [21]

$$\begin{aligned}\mathcal{L} = \bar{\psi}\left[\gamma(i\partial - g_\omega\omega - g_\rho\vec{\rho}\,\vec{\tau} - eA) - m - g_\sigma\sigma\right]\psi \\ + \frac{1}{2}(\partial\sigma)^2 - \frac{1}{2}m_\sigma^2\sigma^2 - \frac{1}{4}\Omega_{\mu\nu}\Omega^{\mu\nu} + \frac{1}{2}m_\omega^2\omega^2 \\ - \frac{1}{4}\vec{R}_{\mu\nu}\vec{R}^{\mu\nu} + \frac{1}{2}m_\rho^2\vec{\rho}^2 - \frac{1}{4}F_{\mu\nu}F^{\mu\nu} \quad (1)\end{aligned}$$

with ψ is Dirac spinor and m is the bare nucleon mass. m_σ, m_ω and m_ρ are meson masses. g_σ, g_ω and g_ρ are the coupling constants and e corresponds to the proton's charge. It vanishes for neutron. $\Omega_{\mu\nu}$, $\vec{R}^{\mu\nu}$, $F_{\mu\nu}$ denote fields tensors.

$$\Omega_{\mu\nu} = \partial^\mu \Omega^\nu - \partial^\nu \Omega^\mu \,, \tag{2}$$

$$\vec{R}^{\mu\nu} = \partial^\mu \vec{\rho}^\nu - \partial^\nu \vec{\rho}^\mu \,, \tag{3}$$

$$F_{\mu\nu} = \partial^\mu A^\nu - \partial^\nu A^\mu \,. \tag{4}$$

The coupling of the σ and ω mesons to the nucleon field reads [21]

$$g_i(\rho) = g_i(\rho_{\text{sat}}) f_i(x) \qquad \text{for} \quad i = \sigma, \omega \tag{5}$$

with the density dependence given by

$$f_i(x) = a_i \frac{1 + b_i(x + d_i)^2}{1 + c_i(x + d_i)^2} \,, \tag{6}$$

where $x = \rho/\rho_{sat}$, ρ is the baryonic density and ρ_{sat} is the baryon density at saturation in symmetric nuclear matter. In eq. (6), the parameters are not independent, but constrained as follows: $f_i(1) = 1$, $f''_\sigma(1) = f''_\omega(1)$, and $f''_i(0) = 0$. These constraints reduce the number of independent parameters for the density dependence.

In the ρ-meson case, we have an exponential density dependence

$$g_\rho(\rho) = g_\rho(\rho_{\text{sat}}) e^{-a_\rho(x-1)} \,. \tag{7}$$

The isovector channel is parametrized by $g_\rho(\rho_{\text{sat}})$ and a_ρ

2.2 The density-dependent point-coupling

The effective Lagrangian density of DD-PC model is defined by [19]

$$\begin{aligned} \mathcal{L} = {} & \bar{\psi}(i\gamma.\partial - m)\psi - \frac{1}{2}\alpha_S(\rho)(\bar{\psi}\psi)(\bar{\psi}\psi) \\ & - \frac{1}{2}\alpha_V(\rho)(\bar{\psi}\gamma^\mu\psi)(\bar{\psi}\gamma_\mu\psi) - \frac{1}{2}\alpha_{TV}(\rho)(\bar{\psi}\vec{\tau}\gamma^\mu\psi)(\bar{\psi}\vec{\tau}\gamma_\mu\psi) \\ & - \frac{1}{2}\delta_S(\partial_\nu\bar{\psi}\psi)(\partial_\nu\bar{\psi}\psi) - e\bar{\psi}\gamma.A.\frac{1-\tau_3}{2}\psi \,. \end{aligned} \tag{8}$$

This Lagrangian contains the isoscalar-scalar interaction (σ meson) $(\bar{\psi}\psi)(\bar{\psi}\psi)$, isoscalar-vector interaction (ω meson) $(\bar{\psi}\gamma^\mu\psi)(\bar{\psi}\gamma_\mu\psi)$, isovector-vector interaction (ρ meson) $(\bar{\psi}\vec{\tau}\gamma^\mu\psi)(\bar{\psi}\vec{\tau}\gamma_\mu\psi)$ and their corresponding gradient couplings $\partial_\nu(...)\partial^\nu(...)$. It also contains the free-nucleon Lagrangian, the point-coupling interaction terms and the coupling of protons to the electromagnetic field. The

derivative terms in eq. (8) account for the main effects of finite range interactions which are important for a quantitative description of nuclear density distribution.

The functional form of the couplings is given by

$$\alpha_i(\rho) = a_i + (b_i + c_i x)e^{-d_i x} \qquad \text{for} \quad i = S, T, TV\,. \tag{9}$$

where $x = \rho/\rho_{\text{sat}}$ and ρ_{sat} denotes the nucleon density in units of the saturation density of symmetric nuclear matter. For more details see Ref. [21]

3 Numerical Details

This work is realized by using the relativistic Hartree-Bogoliubov (RHB) theory based on the DD-ME2 and DD-PC1 parametrizations and separable pairing within the DIRHB computer code [21], in which the RHB equations can be solved iteratively in a basis of spherical, axially symmetric or triaxial harmonic oscillator (HO).

In the present work, we have used the finite range pairing interaction separable in coordinate space which was proposed by Tian et al. [22]. It is given in the pp-channel by

$$V^{pp}(\mathbf{r_1}, \mathbf{r_2}, \mathbf{r'_1}, \mathbf{r'_2}) = -G\delta(\mathbf{R} - \mathbf{R}')P(r)P(r')\,, \tag{10}$$

where $\mathbf{R} = \frac{1}{2}(\mathbf{r_1} + \mathbf{r_2})$ is the centre of mass, $\mathbf{r} = \mathbf{r_1} - \mathbf{r_2}$ are the relative coordinates and $P(r)$ represents the form factor which is given by

$$P(r) = \frac{1}{(4\pi a^2)^{3/2}} e^{-\frac{r^2}{4a^2}}\,. \tag{11}$$

The two parameters: the pairing strength G and the pairing width a have been adjusted to reproduce the density dependence of the gap at the Fermi surface. The following values: $G = 728$ MeV.fm^3 and $a = 0.6442$ fm which were determined for the D1S parametrization [22] of the Gogny force have also been used here. The numbers of Gauss-Laguerre N_{GL} and Gauss-Hermite N_{GH} mesh-points were $N_{\text{GL}} = N_{\text{GH}} = 48$, and the number of Gauss-Legendre mesh-points was $N_{\text{GLEG}} = 80$.

In order to study the convergence of the RHB results in nuclei under investigation, we have calculated the total binding energy as functions of the shells number for the fermions N_{F} for the neutron-rich ^{100}Zn, ^{102}Ge, ^{104}Se, ^{106}Kr, ^{108}Sr, ^{110}Zr, ^{112}Mo and ^{114}Ru nuclei ($N = 70$ isotones). As one can see in Figure 1, the total binding energy converges exactly at $N_{\text{F}} = 10$. That is why all calculations performed with the DIRHB code are carried out in a safe full anisotropic basis of $N_{\text{F}} = 10$. For the bosons, the number of shells is fixed to $N_{\text{B}} = 20$. The β_2-deformation parameter for the harmonic oscillator basis as well as for the initial Woods-Saxon potential is set to 0, except for constrained

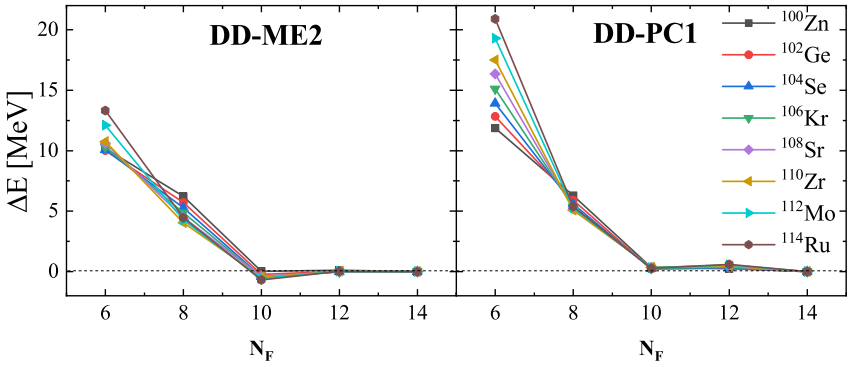

Figure 1. (Color online) Binding Energy difference between a reference calculation performed with 14 shells and calculations performed with $N_{\rm F}$ shells for the $N = 70$ isotones ($30 \leq Z \leq 44$) by using the DD-ME2 and DD-PC1 parametrizations.

calculations of the potential energy surface where the β_2 parameter varies in a range from -0.5 to 0.5 in steps of 0.05. The γ parameter is chosen as free. The different parameter sets of DD-ME2 and DD-PC1 relativistic energy functionals are given in Table 1.

Table 1. The different parameter sets of DD-ME2 [20] and DD-PC1 [19] interactions.

Parameter	**DD-ME2** [20]	**Parameter**	**DD-PC1** [19]
m (MeV)	939	m (MeV)	939
m_σ (MeV)	550.124	a_σ (fm^2)	-10.04616
m_ω (MeV)	783.000	b_σ (fm^2)	-9.15042
m_ρ (MeV)	763.00	c_σ (fm^2)	-6.42729
m_δ (MeV)	0.000	d_σ	1.37235
g_σ	10.5396	a_ω (fm^2)	5.91946
g_ω	13.0189	b_ω (fm^2)	8.86370
g_ρ	3.6836	b_ρ (fm^2)	1.83595
g_δ	0.000	d_ρ	0.64025
a_σ	1.3881		
b_σ	1.0943		
c_σ	1.7057		
d_σ	0.4421		
e_σ	0.4421		
a_ω	1.3892		
b_ω	0.9240		
c_ω	1.4620		
d_ω	0.4775		
e_ω	0.4775		
a_ρ	0.5647		

4 Results and Discussion

4.1 Fermi Levels

As pointed out in the introduction, the choice of studied nuclei, namely: Ge, Se, Kr and Sr, was not random but was based on the study of all nuclei throughout the periodic table. The analysis has shown that $N = 70$ did not behave as a strong magic number except in the selected ones. Figure 2 exhibits the Fermi levels of the selected nuclei as well as those laying in their vicinity around $N = 70$ (i.e. $N = 70$ isotones). In all these nuclei, the well-known magic number $N = 50$ has been reproduced by both models (DD-ME2 and DD-PC1), as there is an abrupt jump in the Fermi levels. The same trend is observed around N=70 except for some nuclei. In Ge, Se, Kr and Sr nuclei, the jumps in Fermi levels strongly support $N = 70$ as a shell closure for both functionals (DD-ME2 and DD-PC1). Above Sr nucleus, this gap becomes more and more weak with increasing protons number Z until quenching in agreement with the results of Ref. [23]. This is more clear with the DD-PC1 expectations. Below Ge nucleus, the relative position of the neutron drip line is located under $N = 70$, as shown in Figure 2. Due to all these considerations, we have restricted our study of the shape evolution at $N = 70$ to the four indicated nuclei (Ge, Se, Kr and Sr) which are investigated in the following section using the potential energy surface quantity.

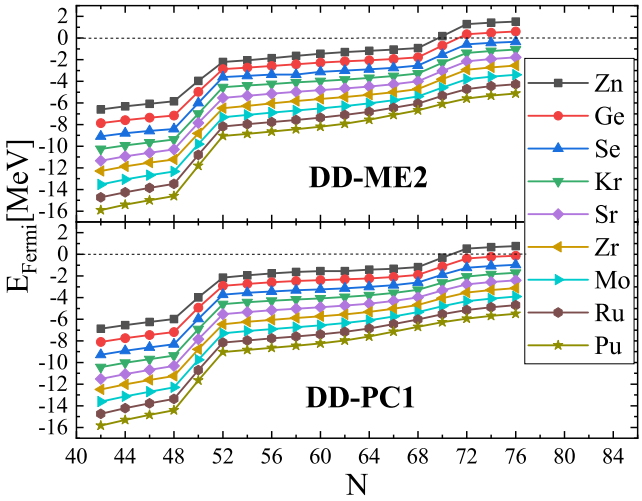

Figure 2. (Color online) The calculated Fermi levels in even-even isotopes with $(30 \leq Z \leq 44)$ using the DD-PC1 and the DD-ME2 sets.

4.2 Potential energy surface

The potential energy surface (PES) represents the difference between the ground state energy and the energy at the deformation parameter β_2. Here, by using the triaxial DIRHB program, we have performed constrained calculations to extract the evolution of the (PES) with the quadrupole moment β_2 which varies in a range from $\beta_2 = -0.5$ to $\beta_2 = 0.5$ in steps of 0.05, as shown in Figure 3. We let the γ parameter free, and we have chosen PES $= 0$ as a position to the ground state. The minimum of PES gives us an idea about the shape of nuclei; if it is attained at $\beta_2 < 0$, the nucleus has an oblate shape; if it is reached at $\beta_2 > 0$, the nucleus form is prolate; if it is reached at $\beta_2 = 0$, the nucleus is spherical.

Aiming to corroborate the previous results that predicted N=70 as a neutron shell closure, we have plotted the Figure 3 which depicts the evolution of potential energy surface (PES) curves of Ge, Se, Kr and Sr isotones for $N = 70$ (middle part of Figure 3) and their neiboring isotones with $N = 68$ (left part of Figure 3) and $N = 72$ (right part of Figure 3) as functions of the quadrupole deformation β_2. From this figure, it is remarkable that both DD-ME2 and DD-PC1 sets generally present the same behaviour. In all $N = 70$ isotones, DD-ME2 and DD-PC1 show a sharp single minimum around the ground state, which confirms

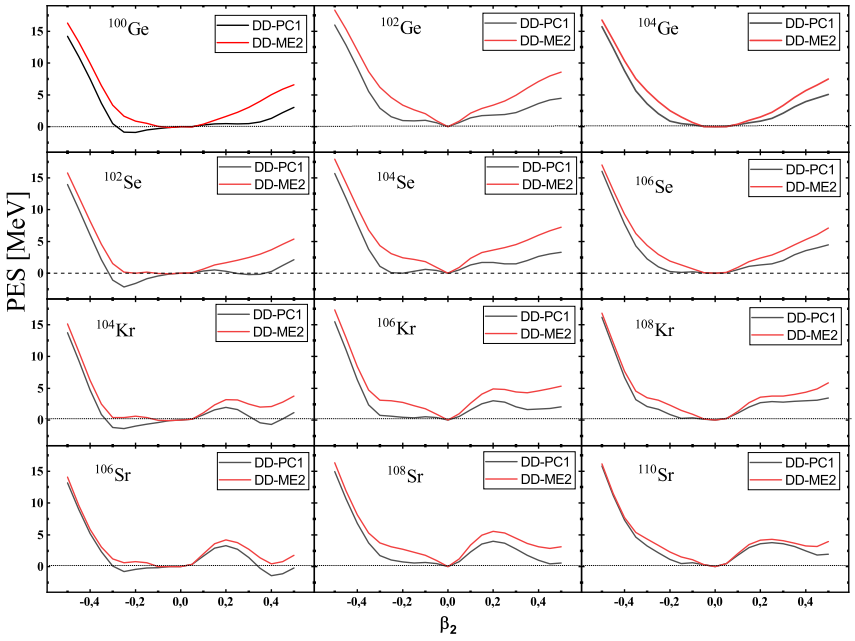

Figure 3. (Color online) The calculated potential surface energy for even-even Ge, Se, Kr and Sr nuclei calculated in RHB with DD-PC1 and DD-ME2 sets.

that the ground states of these isotones are spheric. Furthermore to their spheric ground states, the DD-PC1 potential curves for Se and Kr display wide and flat minima on the oblate side. For $N = 68$ isotones, both models predict an oblate ground state for Se, Kr and Sr and an almost spherical, but slightly oblate ground state for Ge, Se, Kr and Sr $N = 72$ isotones. For ^{100}Ge, solely DD-ME2, predicts an oblate form, whereas DD-PC1 exhibits a flat minima toward the oblate region. Again, with potential surface energy we arrive to prove the magicity in the investigated nuclei at neutron gap $N = 70$.

5 Conclusion

To sum up, even-even neutron rich Ge, Se, Kr and Sr nuclei have been investigated within the covariant density functional theory (CDFT) with DD-PC1 and DD-ME2 parametrizations. The potential energy surface (PES) shows that the four investigated nuclei have a spherical shape at $N = 70$ and predicts that there is a competition between oblate and prolate shapes for $N = 68$. However, the shape of nuclei with $N = 72$ is predicted to be spherical, within DD-ME2 and DD-PC1, Except for Se where the DD-PC1 suggests that this nucleus is oblate. From the Fermi levels, we have found that the neutron drip-line for the four selected nuclei is speculated to be above $N = 70$.

References

[1] B. S. Pudliner et al. (1995) Quantum Monte Carlo calculations of A$\leq$ 6 nuclei. *Phys. Rev. Lett.* **74** 4396 DOI: https://doi.org/10.1103/PhysRevLett.74.4396.

[2] G. Hagen et al. (2016) Emergent properties of nuclei from ab initio coupled-cluster calculations. *Phys. Scr.* **91** 063006 DOI: https://doi.org/10.1088/0031-8949/91/6/063006.

[3] B.R. Barrett et al. (2013) Ab initio no core shell model. *Prog. Part. Nucl. Phys.* **69** 131 DOI: https://doi.org/10.1016/j.ppnp.2012.10.003.

[4] J.E. Drut et al. (2010) Toward ab initio density functional theory for nuclei. *Prog. Part. Nucl. Phys.* **64** 120 DOI: https://doi.org/10.1016/j.ppnp.2009.09.001.

[5] M. Horoi et al. (1994) Truncation method for shell model calculations. *PhysRevC* **50 (5)** R2274 DOI: https://doi.org/10.1103/PhysRevC.50.R2274.

[6] D. Vautherin., and M. Veneroni. (1969) A Hartree-Fock calculation of 208Pb in coordinate space. *Phys. Lett.* **29B** 203 DOI: https://doi.org/10.1016/0370-2693(69)90140-3.

[7] D. Vautherin, and D. M. Brink. (1972) Hartree-Fock Calculations with Skyrme's Interaction. I. Spherical Nuclei. *Phys. Rev. C* **5** 626 DOI: https://doi.org/10.1103/PhysRevC.5.626.

[8] M. El Adri, M. Oulne. (2021) Tensor Force Effect on the Neutron Shell Closure in Super-heavy Elements. *Eur. Phys. J. Plus* **136** 343 DOI: https://doi.org/10.1140/epjp/s13360-021-01328-9.

[9] J. Dechargé, and D. Gogny. (1980) Hartree-Fock-Bogolyubov calculations with the D1 effective interaction on spherical nuclei. *Phys. Rev. C* **21** 4 1568 DOI: https://doi.org/10.1103/PhysRevC.21.1568.

[10] J. D. Walecka. (1974) A theory of highly condensed matter. *Ann. Phys.* **83** 491 DOI: https://doi.org/10.1016/0003-4916(74)90208-5.

[11] Boguta, J., and A. R. Bodmer. (1977) Relativistic calculation of nuclear matter and the nuclear surface. *Nucl. Phys. A* **292** 413 DOI: https://doi.org/10.1016/0375-9474(77)90626-1.

[12] T. Nikšić , D. Vretenar, and P. Ring. (2011) Relativistic nuclear energy density functionals: Mean-field and beyond. *Prog. Part. Nucl. Phys.* **66** 519 DOI: https://doi.org/10.1016/j.ppnp.2011.01.055.

[13] S. E. Agbemava, A. V. Afanasjev, T. Nakatsukasa, and P. Ring. (2015) Covariant density functional theory: Reexamining the structure of superheavy nuclei. *phys. Rev. C* **92** 054310 DOI: https://doi.org/10.1103/PhysRevC.92.054310.

[14] Y. El Bassem, M. Oulne. (2019) Nuclear structure investigation of even-even Sn isotopes within the covariant density functional theory. *phys. Rev. C* **987** 16-28 DOI: https://doi.org/10.1016/j.nuclphysa.2019.04.003.

[15] M. El Adri, M. Oulne. (2020) Neutron shell closure at N = 32 and N = 40 in Ar and Ca isotopes. *Eur. Phys. J. Plus* **135** 268 DOI: https://doi.org/10.1140/epjp/s13360-020-00277-z.

[16] M. El Adri, M. Oulne. (2020) Shell Evolution in Neutron-rich Ge, Se, Kr and Sr Nuclei within RHB Approach. *IJMPE* **29** 12 2050089 DOI: https://doi.org/10.1142/S0218301320500895.

[17] S. Sharma, R. Devi and S.K. Khosa. (2019) Microscopic study of evolution of shape change across even-even mass chain of tellurium isotopes using relativistic Hartree-Bogoliubov model. *Nucl. Phys. A* **988** 12 9-23 DOI: doi.org/10.1016/j.nuclphysa.2019.05.008.

[18] T. A. Siddiqui et al. (2020) A search for neutron magicity in the isotopic series of Z = 122, 128 superheavy nuclei. *J. Phys. G: Nucl. Part. Phys.* **47** 11 DOI: https://doi.org/10.1088/1361-6471/ab8914.

[19] T. Nikšić, D. Vretenar, and P. Ring. (2008) Relativistic nuclear energy density functionals: Adjusting parameters to binding energies. *Phys. Rev. C* **78** 034318 DOI: https://doi.org/10.1103/PhysRevC.78.034318.

[20] G. A. Lalazissis, T. Nikšić , D. Vretenar, and P. Ring. (2005) New relativistic mean-field interaction with density-dependent meson-nucleon couplings. *Phys. Rev. C* **71** 024312 DOI: https://doi.org/10.1103/PhysRevC.71.024312.

[21] T. Nikšić, N. Paar, D. Vretenar et P. Ring. (2014) DIRHB—A relativistic self-consistent mean-field framework for atomic nuclei. *Comput. Phys. Commun.* **185** 1808-1821 DOI: https://doi.org/10.1016/j.cpc.2014.02.027.

[22] Y. Tian, and Z. Y. Ma, P. Ring. (2009) A finite range pairing force for density functional theory in superfluid nuclei. *Phys. Lett. B* **676** 44 DOI: https://doi.org/10.1016/j.physletb.2009.04.067.

[23] M. Bender, et al. (2009) Tensor part of the Skyrme energy density functional. II. Deformation properties of magic and semi-magic nuclei. *Phys. Rev. C* **80** 6 064302 DOI: https://doi.org/10.1103/PhysRevC.80.064302.